ELSEVIER

Applied Surface Science 92 (1996) 571–574

applied surface science

Light emission from the porous boron δ-doped Si superlattice

Ting-Chang Chang [a,*], Wen-Kuan Yeh [b], Ming-Yuh Hsu [b], Chun-Yen Chang [b], Chien-Ping Lee [b], Tz-Guei Jung [b], Wen-Chung Tsai [b], Guo-Wei Huang [b], Yu-Jane Mei [b]

[a] *National Nano Device Laboratory, 1001-1 Ta-Hsueh Rd., Hsin-Chu 30050, Taiwan, ROC*

[b] *Department of Electronics Engineering and Institute of Electronics, National Chiao Tung University, Hsin-Chu 300, Taiwan, ROC*

Received 12 December 1994; accepted for publication 4 March 1995

Abstract

We report the first study on the porous boron δ-doped Si superlattice. Visible photoluminescence (PL) was observed with multiple peaks from the porous boron δ-doped Si superlattice at room temperature. In the electroluminescence (EL) experiment, a bright yellow light emission was observed from the porous boron δ-doped Si superlattices. However, a weak red light emission was also observed from the conventional porous Si which is anodized at the same etching condition. As a result, the structure of the porous boron δ-doped Si superlattice has the ability of controlling the quantum size in porous Si and enhancing the light intensity from porous Si.

1. Introduction

The band structure of silicon has an indirect bandgap of 1.1 eV. Therefore, there is no optical recombination of excited states in bulk silicon in the visible region. As a consequence, light-emitting devices have to be made with a different substrate, e.g., GaAs. This is a technological drawback since the silicon technology is well established and comparatively cheap. A possible light emission of silicon is of extreme practical importance. First, a number of new processes and devices are possible. If a light-emitting device can be monolithically integrated with other structures on silicon, a big step in micro-optics, photon data transmission, and processing can be achieved.

A possible attempt to get light emission out of silicon is to use nanocrystalline structures. When the size of the silicon structures is very small, direct optical recombination is no longer impossible. One way towards nanocrystalline structures is the formation of porous silicon [1,2]. This is done by partial anodic dissolution of silicon in HF. This process produces a film with high porosity and a very thin remaining structure. Porous silicon was used previously in silicon technology in order to fabricate silicon-on-insulator structures [3]. It is compatible with the CMOS process.

The origin and mechanism of visible photoluminescence (PL) in porous Si are not yet understood and several models have been suggested. One model is that the quantum-confinement effect in Si nanocrystallines enhances the oscillator strength of the direct optical transitions and gives efficient radiations from porous Si [4–7]. On the other hand, with a large surface-to-volume ratio in the high porous

* Corresponding author. Tel.: +886 35 726100 Ext 7710; fax: +886 35 713403.

SSDI 0169-4332(95)00297-9

structure, surface localized states in Si nanocrystallines are considered to be responsible for the origin of luminescence of porous Si [8–10]. Moreover, silicon-based compounds such as siloxene ($Si_6O_3H_6$) derivatives [11] or rearranged Si–Si bonds like small H-terminated Si clusters [12] formed at the surface are also proposed as an origin of the strong PL of porous Si. Now, the popular model is the quantum-confinement effect model. Due to the small dimensions in the range of the De Broglie wavelength, the effective bandgap is estimated to be increased by quantum confinement so that the emitted wavelength could be shifted from the infrared into the visible range. It is supposed that a reduction of feature size of the crystallites would further decrease the emitted wavelength.

Controlling and understanding the visible luminescence in porous Si may open the possibility to make it as one of the most important optoelectronic materials in the future. In this work, we study for the first time the possibility of artificially controlling the quantum size in the porous state via anodizing epitaxial superlattices.

2. Experimental

The epitaxial boron δ-doped Si superlattice was grown on 10 Ω · cm, p-type, (001) Si substrates using a home-made hot-wall multiwafer Ultrahigh Vacuum/Chemical Vapor Deposition (UHV/CVD) system. The growth temperature was kept constant at 550°C. Prior to the growth, the substrate was subjected to an $H_2SO_4 : H_2O_2 = 3 : 1$ clean and a 10% HF dip. Silane (SiH_4) was used as a reactant gas. In addition, 1% diborane (B_2H_6) in hydrogen was used as the p-type dopant gas. The base pressure of the system was maintained at about 2×10^{-8} Torr in the growth chamber. During growth, the system was operated at about 1.0 mTorr. The porous boron δ-doped Si superlattice was formed by anodization of the as-grown boron δ-doped Si superlattice in a HF–ethanol solution ($HF : C_2H_5OH : H_2O = 1 : 1 : 2$) at a current density of 12.5 mA/cm^2. A platinum wire was used for the cathode of the electrolytic cell. Before anodization, the as-grown superlattice was cleaned, and an ohmic contact was formed by evaporating a thin Al film onto the back surface to ensure a uniform anodic current distribution. The structure of the porous superlattice was examined by a Hitachi S2000 SEM with a spatial resolution of 1.8 nm at 30 kV. High-resolution double-crystal X-ray diffraction (HRXRD) was employed for determining the structural parameters of the as-grown superlattice. The PL measurement was performed with a 1 m monochromator and a photomultiplier in conjunction with standard lock-in techniques while the sample was excited by the 514 nm line of an unfocussed argon ion laser.

3. Results and discussion

In Fig. 1, curve (a) shows a HRXRD rocking curve for the as-grown boron δ-doped Si superlattice grown on (001) Si substrate. This superlattice consisted of 51 periods of boron δ-doped Si. In this figure, the peak Sub represents the Si substrate reflection, peak P0 the zeroth-order superlattice reflection, and other main peaks are nth-order satellite peaks (−2, −1, +1, +2), resulting from the periodicity of the superlattice. Curve (b) represent the simulated rocking curve for a Si/Si–B superlattice of 51 periods with the Si layer 28 nm thick and the Si–B layer 3.1 nm thick with a boron concentration of 1.75×10^{20} cm^{-3}. When compared to curve (a), good matches between experiment and simulation in

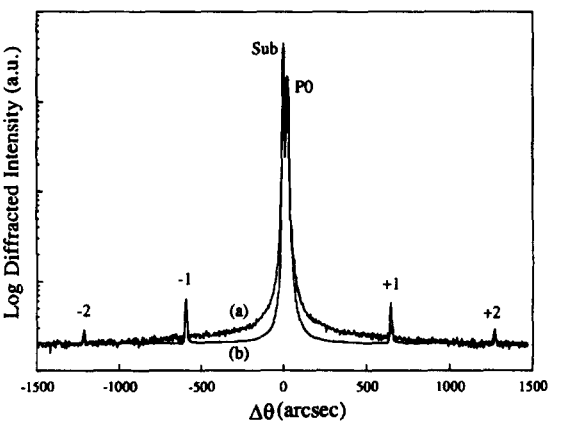

Fig. 1. (a) HRXRD rocking curve for boron δ-doped Si superlattice grown on (001) Si substrate; (b) simulated rocking curve for a Si/Si–B superlattice of 51 periods with the Si layer 28 nm thick and the Si–B layer 3.1 nm thick with a boron concentration of 1.75×10^{20} cm^{-3}.

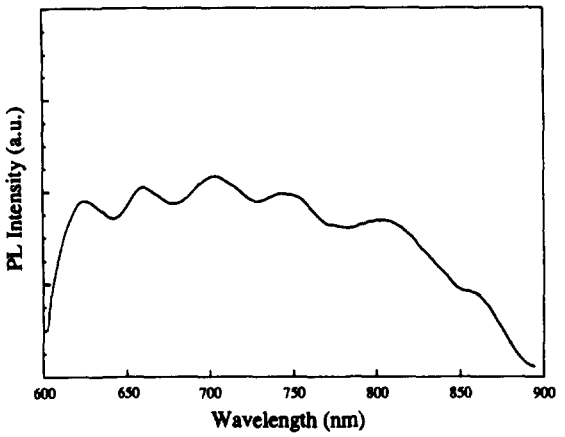

Fig. 2. Room temperature photoluminescence spectrum of the porous boron δ-doped Si superlattice. Multiple peaks were observed in this spectrum.

terms of peak position and peak intensity of each main peak are clearly observed. Therefore, boron δ-doped Si superlattice with high crystalline quality could be achieved by UHV/CVD [13–15].

Fig. 2 shows the room temperature PL spectrum of the porous boron δ-doped Si superlattice. Visible photoluminescence with multiple peaks was observed from this novel structure. This result is very different from that of the conventional porous Si. In conventional porous Si, only one peak was observed. In contrast to this, six peaks were observed in the porous boron δ-doped Si superlattice. The multiple peaks of the PL spectrum from the porous boron δ-doped Si superlattice can be explained on the basis of interference from the periodic structure [16].

Fig. 3 shows a typical cross-sectional SEM micrograph of this porous boron δ-doped Si superlattice. The layered structures of the porous boron δ-doped Si superlattice were clearly observed. The period of thickness was measured to be 31 ± 2 nm. This value agrees with that of the as-grown boron δ-doped Si superlattice.

Figs. 4a and 4b show the photographs of light

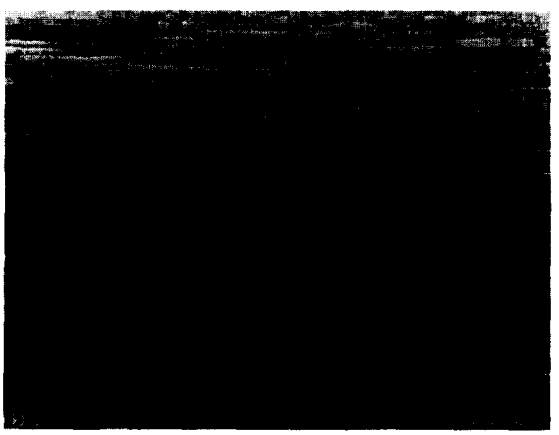

Fig. 3. Cross-sectional SEM micrograph of the porous boron δ-doped Si superlattice.

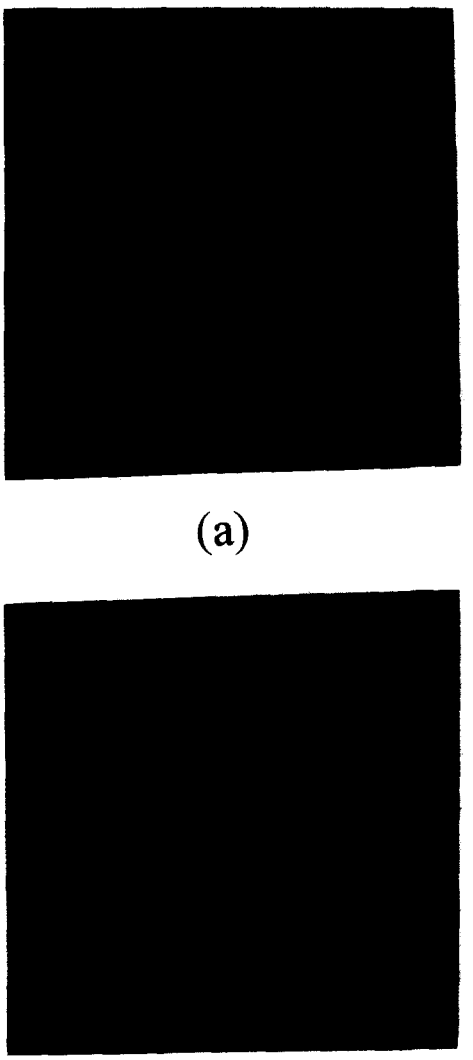

Fig. 4. Photograph of light emission from the EL devices of the conventional porous Si (a) and the porous boron δ-doped Si superlattice (b).

emission from the electroluminescence (EL) devices of the conventional porous Si and the porous boron δ-doped Si superlattice, respectively. For the conventional porous Si, a dark red light was emitted, as shown in Fig. 4a. On the other hand, a bright yellow light emission was observed from the porous boron δ-doped Si superlattice. The emitted light intensity of the porous boron δ-doped Si superlattice is greater than that of the conventional porous Si, indicating that the structure of the porous boron δ-doped Si superlattice can enhance the quantum efficiency of EL. In terms of the wavelength of emitted light, the EL device of the porous boron δ-doped Si superlattice emits a light with shorter wavelength. According to the quantum size model for porous Si, the shorter wavelength of emitted light corresponds to a device with smaller size of Si crystallites. As a result, the structure of the porous boron δ-doped Si possibly has the ability of controlling and reducing the quantum size of porous Si. However, the result of EL contradicts the result of PL. Fig. 2 shows the PL of the porous boron δ-doped Si superlattice. The wavelength of PL ranges from 620 to 850 nm. The corresponding color of PL is red and near-IR; however, the light color of EL is yellow. The difference between the photoluminescence and the electroluminescence may be due to a different emission mechanism. It has been proposed that the origin of photoluminescence is associated with surface effects, and quantum effects may be responsible for the electroluminescence [17]. Very recent data [17], show a fast ($\tau \approx 10$ ns) blue component of the photoluminescence signal, which is identified as the direct recombination in the crystallites interior, whereas the main (97%) fraction of the photoluminescence signal stems from slow red ($\tau \sim \mu$s to ms) radiative transitions in the surface of crystallites. This gives us reason to believe that via electrical excitation the shorter wavelength radiative recombination channel in the core of the crystallites is preferred in contrast to the longer wavelength surface recombination channel in the optical excited case. Therefore, the inconsistency between PL and EL can be explained on the basis of different mechanisms.

4. Conclusions

In this work, we report the first study on the porous boron δ-doped Si superlattice. Visible photoluminescence (PL) was observed with multiple peaks from the porous boron δ-doped Si superlattice at room temperature. In the electroluminescence (EL) experiment, a bright yellow light emission was observed from the porous boron δ-doped Si superlattices. However, a weak red light emission was also observed from the conventional porous Si which is anodized at the same etching condition. As a result, the structure of the porous boron δ-doped Si superlattice is able to enhance the light intensity of porous Si.

Acknowledgement

This work was performed at National Nano Device Laboratory which was supported in part by the National Science Council of the Republic of China under contract No. NSC 82-0404-E009-233 & NSC 85-2721-2317-001.

References

[1] R. Bemming and G. Schwandt, Surf. Sci. 4 (1966) 109.
[2] M.I.J. Beale, J.D. Benjamin, M.J. Uren, M.I.J. Chew and A.G. Cullis, J. Cryst. Growth 73 (1985) 662.
[3] G. Bomchil, A. Halimaoui and R. Herino, Microelectron. Eng. 8 (1988) 293.
[4] S. Gardelis, Appl. Phys. Lett. 59 (1991) 2118.
[5] R. Tsu, H. Shen and M. Dutta, Appl. Phys. Lett. 60 (1992) 112.
[6] T. Ohno, K. Shiraishi and T. Ogawa, Phys. Rev. Lett. 69 (1992) 2400.
[7] T. Takagahara and K. Takeda, Phys. Rev. B 46 (1992) 15578.
[8] M.A. Tischler, R.T. Collins, J.H. Stathis and J.C. Tsang, Appl. Phys. Lett. 60 (1992) 639.
[9] C. Tsai, Appl. Phys. Lett. 60 (1992) 1700.
[10] T. George et al., Appl. Phys. Lett. 60 (1992) 2359.
[11] M.S. Brandt et al., Solid State Commun. 81 (1992) 307.
[12] Y. Kanemitsu et al., Appl. Phys. Lett. 61 (1992) 2446.
[13] T.C. Chang, C.Y. Chang, T.G. Jung and W.C. Tasi, J. Appl. Phys. 75 (1994) 3441.
[14] T.C. Chang, C.Y. Chang, T.G. Jung and W.C. Tasi, Jpn. J. Appl. Phys. 33 (1994) 1787.
[15] T.C. Chang, C.Y. Chang, T.G. Jung and W.C. Tasi, in: Proc. 7th Int. MicroProcess Conf. (1994) p. 262.
[16] T.C. Chang, C.Y. Chang, T.G. Jung and W.C. Tasi, in: Proc. Int. Electron Devices and Materials Symp. (1994) p. 2-2-5.
[17] P.D.J. Calcott, K.J. Nash, L.T. Canham, M.J. Kane and K. Brumhead, J. Phys.: Condens. Matter 5 (1993) L91.